Cerebellum (2015) 14:516–527
DOI 10.1007/s12311-015-0673-9

ORIGINAL PAPER

α-Synuclein Expression in the Mouse Cerebellum Is Restricted to VGluT1 Excitatory Terminals and Is Enriched in Unipolar Brush Cells

Sun Kyong Lee[1] · Roy V. Sillitoe[2] · Coralie Silva[1] · Marco Martina[1] · Gabriella Sekerkova[1]

Published online: 28 April 2015

Abstract α-Synuclein has a crucial role in synaptic vesicle release and synaptic membrane recycling. Although its general expression pattern has been described in the cerebellum, the precise cerebellar structures where α-synuclein is localized are poorly understood. To address this question, we used α-synuclein immunohistochemistry in adult mice cerebellar sections. We found that α-synuclein labels glutamatergic but not glycinergic and GABAergic synaptic terminals in the molecular and granule cell layers. α-Synuclein was preferentially expressed in parallel and mossy fiber synaptic terminals that also express vesicular glutamate transporter 1 (VGluT1), while it was not detected in VGluT2-positive climbing fibers. α-Synuclein was particularly enriched in lobules IX and X, a region known to contain a high density of unipolar brush cells (UBCs). To elucidate whether the α-synuclein-positive mossy fibers belong to UBCs, we double-labeled cerebellar sections with antibodies to α-synuclein and UBC-type-specific markers (calretinin for type I and metabotropic glutamate receptor 1α (mGluR1α) for type II UBCs) and took advantage of organotypic cerebellar cultures (in which all mossy fibers are UBC axons) and moonwalker mice (in which almost all UBCs are ablated) and found that both type I and type II UBCs express α-synuclein. In moonwalker mutant cerebella, the α-synuclein/VGluT1 immunolabeling showed a dramatic decrease in the vestibulocerebellum that correlated with the absence of UBC. α-Synuclein appears to be an excellent marker for intrinsic mossy fibers of the VGluT1 subset in conjunction with UBCs of both subtypes.

Keywords VGluT1 · VGluT2 · Granule cells · Moonwalker mice · Mossy fiber terminals · Vestibulocerebellum

Introduction

α-Synuclein function may be central to the pathogenesis of several neurodegenerative diseases, including Parkinson's disease, dementia with Lewy bodies, multiple system atrophy, and Alzheimer's disease [1–6]. The hallmark of these neurodegenerative diseases, collectively termed synucleopathies, is the aggregation of α-synuclein in cytoplasmic deposits such as the Lewy bodies and senile plaques [1, 2]. α-Synuclein is a small, highly conserved presynaptic protein that is enriched in the vertebrate central nervous system (CNS). It plays a role in synaptic transmission and synaptic plasticity under physiological conditions [1, 7–11]. During normal synaptic function, α-synuclein behaves as a nonclassical chaperone for soluble N-ethylmaleimide-sensitive (NSF) protein receptor (SNARE) complex assembly and regulates vesicle trafficking and recycling [9, 12, 13].

α-Synuclein protein [14] and messenger RNA (mRNA) (in situ hybridization (ISH) [15]) are both abundantly and widely expressed in different neuronal populations throughout the CNS. Despite its abundance, the brain expression of the α-synuclein is not ubiquitous, but instead it is rather selective to

This paper is dedicated to the Prof. Enrico Mugnaini, a visionary neuroanatomist and an inspirational mentor.

✉ Gabriella Sekerkova
g-sekerkova@northwestern.edu

[1] Department of Physiology, Feinberg School of Medicine, Northwestern University, Morton 5-619, Chicago, IL 60611, USA

[2] Department of Pathology and Immunology, Baylor College of Medicine, Jan and Dan Duncan Neurological Research Institute of Texas Children's Hospital, Houston, TX 77030, USA

specific neuronal populations [16]. This is especially true for the cerebellum, where expression of α-synuclein transcripts is restricted to the granule cell layer, and no mRNA signal is detectable in Purkinje cells and stellate/basket cells in molecular layer [15]. Remarkably, α-synuclein expression is particularly intense in the vestibulocerebellum, encompassing the nodulus (lobule X), uvula (lobule IX), and flocculus/paraflocculus complex. These cerebellar regions are known to contain a high density of unipolar brush cells (UBCs), a special class of excitatory interneurons [17, 18]. In this study, we investigated the presence of α-synuclein in different cerebellar circuitries, with special emphasis on the UBCs. We used immunohistochemical labeling of cerebellar cryosections as well as in vitro slice cultures of wild-type mouse. Because α-synuclein staining appears in register with regions that contain UBCs, we took advantage of moonwalker (*Mwk*) mice, in which type II UBCs are completely absent [18] to verify that α-synuclein expression is indeed enriched in these neurons.

We found that α-synuclein is associated with excitatory presynaptic terminals and, in particular, with VGluT1-expressing terminals of granule cells and UBCs in the cerebellar cortex and that its expression is dramatically reduced in the *Mwk* mouse. Interestingly, intrinsic mossy fiber terminals (MFTs, the UBC axons) that also express VGluT1 contain much higher levels of α-synuclein than the extrinsic MFTs originating from precerebellar nuclei.

Materials and Methods

Animals and Tissue Preparation

This study was carried out on mice in accordance with the protocols approved by the Northwestern University and Baylor College of Medicine Animal Care and Use Committee. The following mouse strains were used: CD1 as wild type, α-synuclein knockout (α-synuclein KO) (129X1-Sncatm1Rosl/J; Jackson Laboratories), heterozygous moonwalker (*Mwk*/$^{+}$) (ENU-mutagenized mice [19, 20]), and their control littermates.

Adult mice of both sexes (32 to 60 days old, $N=12$) were anesthetized with sodium pentobarbital (60 mg/kg body weight) and then perfused through the ascending aorta with saline followed by freshly depolymerized 4 % paraformaldehyde in 0.12 M phosphate buffer (PB), pH 7.4. One hour after the perfusion, the brains were dissected out and cryoprotected in a series of sucrose solutions in phosphate buffered saline (PBS), 10, 20, and then 30 %. Cryoprotected cerebella were sectioned in the sagittal or coronal planes at 25 μm on a freezing stage microtome and the sections were collected serially in multiwell plates. No differences were observed in the α-synuclein distribution between the 32- and the 60-day-old mice.

Organotypic Cultures

Organotypic cerebellar slice cultures were prepared from postnatal day (P) 8–10 mice as described previously [21]. The mice were euthanized by CO_2 inhalation and then immediately perfused with saline (0.9 % NaCl). Next, the cerebellum was dissected out and sagittally sliced at 250 μm using a McIlwain tissue chopper. Lobule X was isolated from residual meninges in cold 1× Hank's balanced salt solution (HBSS, Life Technologies) and then placed on the membrane surface of Millicell-CM culture plate inserts (Millipore) equilibrated in plating medium (basal medium eagle containing 25 % horse serum, 1/4× HBSS, 1 mM L-glutamine, 0.1 % D-glucose, 1 % penicillin/streptomycin, and 0.05 % fungizone). At 7 days in vitro (DIV), the medium was replaced with maintaining medium (basal medium eagle containing 15 % horse serum, 1/4× HBSS, 1 mM L-glutamine, 0.1 % D-glucose, 1 % penicillin/streptomycin, and 0.05 % fungizone). The medium was changed every 2–3 days and cultures were grown for 22–24 DIV at 37 °C in a humidified atmosphere with 5 % CO_2/95 % O_2. The slices were then fixed for 30 min at room temperature with 4 % paraformaldehyde in 0.12 M PB after which they were kept in PBS at 4 °C.

Immunohistochemistry

Bright-Field Microscopy Cryosections were processed for immunohistochemistry according to an avidin/biotin amplification protocol. Briefly, the endogenous peroxidase activity was blocked in 0.3 % H_2O_2 and 10 % methanol in Tris buffered saline (TBS; 100 mM Tris and 150 mM NaCl; pH 7.4). Nonspecific binding was suppressed in a blocking solution containing 5 % normal goat serum (NGS) and 1 % bovine serum albumin (BSA) in TBS with 0.2 % Triton X-100. Sections were then incubated overnight or up to 2 days at 4 °C with a primary antibody. Bound antibodies were detected using biotinylated anti-mouse, anti-guinea pig, or anti-rabbit IgG (GE Healthcare), ABC Elite kit (Vector Laboratories), and diaminobenzidine (DAB; Sigma). Control sections incubated without primary antibodies were free of immunoreaction products.

Immunofluorescence To study colocalization of different proteins, cryosections and organotypic slice cultures were immunolabeled with a combination of antibodies. Briefly, after 1 h pretreatment with a blocking solution containing 5 % NGS and 1 % BSA in TBS with 0.2 % Triton X-100, the sections were incubated for 2–3 days at 4 °C in a cocktail of primary antibodies raised in different species. Bound primary antibodies were visualized by secondary antibodies coupled to Alexa Fluor 488 or Alexa Fluor 594 (Invitrogen).

Primary Antibodies The following primary antibodies were used: rabbit, mouse, sheep, and guinea pig anti-α-synuclein; mouse and rabbit anti-calretinin; mouse anti-glutamate acid decarboxylase 67 (GAD67); guinea pig anti-glycine transporter 2 (GlyT2); rabbit anti-25-kDa heat shock protein (Hsp25); mouse and rabbit anti-mGluR1α; guinea pig anti-vesicular glutamate transporter 1 (VGluT1); and guinea pig anti-vesicular glutamate transporter 2 (VGluT2). Detailed specifications of these antibodies are listed in Table 1.

Specificity of α-Synuclein Antibodies The specificity of these antibodies was tested on α-synuclein KO mice brain sections (Fig. 1). Two of the three antibodies tested proved to be specific: the monoclonal antibody from EnCor Biotechnology (MCA-3H9) and the sheep polyclonal antibody from Santa Cruz Biotechnology (AB5336) (Fig. 1a, b, e, f). Both these antibodies showed immunostaining (see also Fig. 2a) in brain regions that were previously reported to express α-synuclein either by ISH (see Allen brain atlas [15]) or by immunohistochemistry using a proprietary antibody [14], and there was no staining in brain sections from α-synuclein KO mice (Fig. 1e, f). Surprisingly, the antibody raised in guinea pig (PC325; Calbiochem) proved to be nonspecific as it produced the same staining pattern in the wild-type and α-synuclein KO mice (Fig. 1c, g) and, thus, was not used in the study. Finally, we tested one pan-synuclein antibody raised in rabbit (C0336; Assay Biotech). In the wild-type cerebellum, this antibody showed the same staining pattern as the monoclonal α-synuclein antibody (Fig. 1d); in double-immunolabeled sections, the two antibodies colocalized in the MFTs (Fig. 1i–j). No immunostaining was detected in the cerebellum of the KO mouse (Fig. 1h).

Image Acquisition

Images of cerebellar sections were acquired with a Spot RT CCD video camera (Diagnostic Instruments) mounted on a Nikon Eclipse E800 microscope. Laser scanning confocal images were obtained with a Nikon PCM 2000 Confocal Microscope System using Simple PCI Program. Images were analyzed individually or in z-stacks of different depths. For colocalization experiments, type FF immersion oil was used

Table 1 List of primary antibodies used in this study

Antibody	Species	Dilution	Immunogen	Source	Characterization references
α-Synuclein	Mouse	1:3000	Full-length human protein epitope from amino acids 61–95	EnCor Biotechnology Cat. No.: MCA-3H9	α-Synuclein KO mice[a]
α-Synuclein	Sheep	1:1000	Synthetic peptide corresponding to amino acids 108–120 human α-synuclein	Santa Cruz Biotechnology Cat. No.: AB5336	α-Synuclein KO mice[a]
α-Synuclein	Guinea pig	1:5000	Synthetic peptide corresponding to amino acids 123–140 of the C-terminus rat α-synuclein	Calbiochem Cat. No.: PC325	α-Synuclein KO mice[b]
pan-Synuclein	Rabbit	1:1000	Synthetic peptide derived from human α-synuclein	Assay Biotech Cat. No.: C0336	Colabeling with mouse anti-α-synuclein[c]
Calretinin	Mouse	1:2000	Full-length recombinant human CR	Swant, Switzerland Cat. No.: 6B3	[18]
Calretinin	Mouse	1:1000	Full-length recombinant human CR	Millipore Cat. No.: MAB1568	[36]
Calretinin	Rabbit	1:5000	Full-length recombinant human CR	Swant, Switzerland Cat. No.: 7696/3H	[18]
GAD67	Mouse	1:1000	Recombinant GAD67 protein	Millipore Cat. No.: MAB5406	[22]
GlyT2	Guinea pig	1:5000	Synthetic peptide from the C-terminus as predicted from the cloned rat GlyT2	Millipore Cat. No.: AB1173	[23]
Hsp25	Rabbit	1:500	Recombinant mouse Hsp25 protein	Assay Designs Enzo Life Sciences Cat. No.: SPA-801	[39, 40]
mGluR1α	Mouse	1:800	Fusion protein containing sequences from C-terminus of rat mGluR1α	Pharmingen Cat. No.: 556389	[24]
mGluR1α	Rabbit	1:500	Peptide representing amino acid residues 945–1127 of mouse mGluR1α	Frontier Institute Co, Japan Cat. No.: Rb-Af811-1	[18]
VGLUT1	Guinea pig	1:5000	Synthetic linear peptide from rat VGLUT1 protein	Millipore Cat. No.: AB2251	[29]
VGLUT2	Guinea pig	1:5000	Synthetic linear peptide from rat VGLUT2 protein	Millipore Cat. No.: AB5905	[29]

[a] Sections from SNCA KO mouse labeled with these antibodies showed no immunolabeling (Fig. 1a, b, e, f)

[b] Sections from SNCA KO mouse labeled with these antibodies showed the same immunolabeling as the wild-type animals (Fig. 1c, g)

[c] In cerebellar sections, the rabbit anti-pan-synuclein showed complete colocalization with mouse anti-α-synuclein (Fig. 1i)

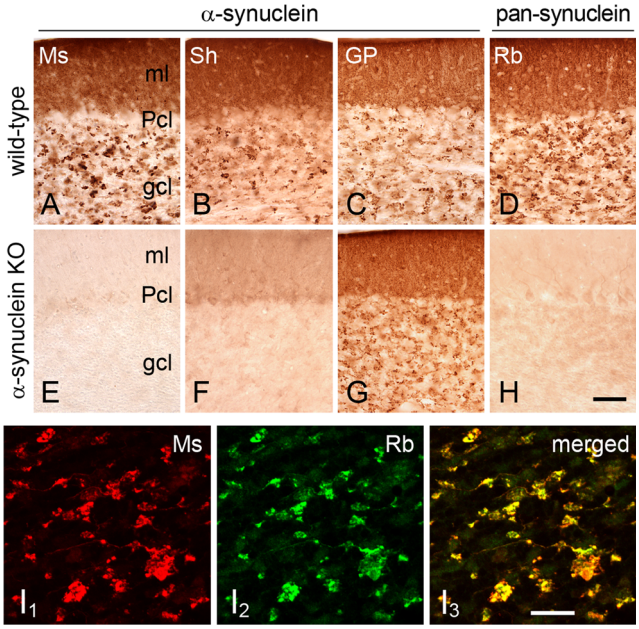

Fig. 1 Specificity of α-synuclein antibodies. Cerebellar cryosections prepared from wild-type (**a**–**d**; **i**) and α-synuclein KO (**e**–**h**) mice immunostained with α-synuclein antibodies raised in mouse (*Ms*; EnCor Biotechnology), sheep (*Sh*; Santa Cruz Biotechnology), and guinea pig (*GP*; Calbiochem) and pan-synuclein antibody raised in rabbit (*Rb*). **a**–**d** In wild-type mice, all the tested antibodies showed a similar staining pattern. A punctate-like immunostaining in the molecular layer (*ml*), MFT staining in the granule cell layer (*gcl*), and no staining in the Purkinje cell layer (*Pcl*). **e**–**h** No immunolabeling is detected in the α-synuclein KO sections using antibodies raised in mouse (**e**), sheep (**f**), and rabbit (**h**). Antibody raised in guinea pig showed the same staining pattern in the α-synuclein KO and the wild-type mouse (**g**). $\mathbf{i}_{1–3}$ Colocalization of mouse anti-α-synuclein and rabbit anti-pan-synuclein antibodies in the same MFTs. *Scale bars*: **a**–**h** 50 μm; $\mathbf{i}_{1–3}$ 20 μm

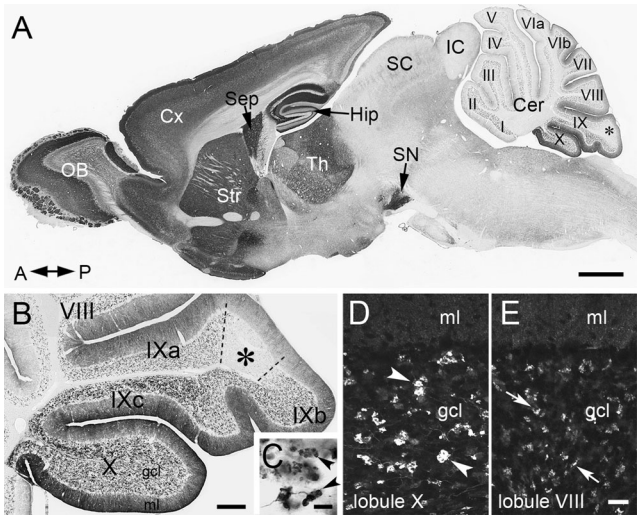

Fig. 2 α-Synuclein immunolabeling in wild-type mouse brain. **a**–**c** Parasagittal cryosection labeled with an immunoperoxidase protocol using mouse anti-α-synuclein antibody (EnCor Biotechnology). **a** Intense immunolabeling is present in the forebrain structures: olfactory bulb (*OB*), cortex (*Cx*), septum (*Sep*), striatum (*Str*), hippocampus (*Hip*), and thalamus (*Th*). The midbrain and the hindbrain contain very little immunostaining with the exception of the substantia nigra (*SN*) and cerebellum (*Cer*). In the cerebellum, α-synuclein show a distinct pattern, with more intense immunolabeling in the posterior cerebellum (*lobules VIb–X*) than in the anterior cerebellum (*lobules I–VIa*). The UBC free zone (*asterisk*) is not labeled with α-synuclein antibody. *SC* superior colliculus, *IC* inferior colliculus. Anterior (*A*) and posterior (*P*) directions are indicated by the *double-headed arrow*. **b** α-Synuclein immunostaining in the nodulus (*lobule X*) and uvula (*lobule IX*) shows intense immunostaining in the granule cell layer (*gcl*) of nodulus and folium IXc. In folium IXb, the immunolabeling is less intense; folium IXa and lobule VIII show only moderate immunostaining. The *gcl* in the transition zone between IXa and IXb contains no α-synuclein immunolabeling (*asterisks*; area delineated with *dashed lines*). *ml* molecular layer. **c** α-Synuclein$^+$ MFTs in gcl of nodulus (*arrowheads*). **d**, **e** Comparison of α-synuclein immunolabeling between lobule X and VIII; immunofluorescence staining using mouse anti-α-synuclein antibody. The MFTs (*arrowheads*) in gcl of lobule X are clearly recognizable by intense α-synuclein immunolabeling. In lobule VIII, the α-synuclein$^+$ MFTs (*arrows*) are smaller and with moderate immunolabeling. *Scale bars*: **a** 1 mm; **b** 200 μm; **c** 10 μm; **d**, **e** 20 μm

with either a ×40 plan-fluor lens (numerical aperture 1.3) or a ×60 plan-apochromatic lens (numerical aperture 1.4). To minimize channel spillover, the images were sequentially acquired. All images were processed with Adobe Photoshop CS5. Brightness and contrast were adjusted.

Results

α-Synuclein in the Cerebellar Cortex

While α-synuclein inclusions are the hallmark of diffuse Lewy body disease, including Parkinson's, they are also the hallmark of multiple system atrophy-cerebellar (MSA-C), a cause of adult onset cerebellar ataxia [3, 25] in which the CSF appears particularly favorable to α-synuclein aggregation [26]. Despite the evidence pointing to the cerebellum as an important target of synucleinopathies, the normal distribution of α-synuclein in the cerebellum has not been thoroughly investigated. We studied wild-type mouse brain in sections immunolabeled with commercially available α-synuclein antibodies (Table 1, Fig. 1).

In wild-type animals, intense staining was observed in forebrain regions, including the olfactory bulb, cortex, hippocampus, septum, striatum, and thalamus. The mesencephalon and the hindbrain showed very little immunostaining with the exception of the substantia nigra (Fig. 2a). The cerebellum showed a distinct immunostaining pattern that is described in detail below (Fig. 2a, b). α-Synuclein immunostaining was strictly associated with neurons, most specifically with axonal terminals (Fig. 2c–e); glial cells were not labeled.

α-Synuclein antibodies revealed a distinct staining pattern in the cerebellar cortex (Fig. 2a, b). The posterior cerebellum, especially the vestibulocerebellum (nodulus and uvula), showed intense immunolabeling, while the immunolabeling

of the anterior cerebellum was moderate to faint. In both areas, the immunostaining was localized to fibers and presynaptic terminals in the molecular and granule cell layers (Fig. 2b–e). We did not detect staining in the somata of any cerebellar neurons. To further identify the terminals displaying α-synuclein labeling, we employed double immunolabeling using cell-type-specific antibodies recognizing different cerebellar markers. VGluT1 and VGluT2 were used to identify excitatory glutamatergic terminals of the granule cells and climbing fibers, respectively, in the molecular layer, as well as MFTs in the granule cell layer [27–29]. GAD67 immunolabeling was used to identify inhibitory terminals of GABAergic neurons including Purkinje cells, Golgi cells, stellate cells, and basket cells [30]. Finally, GlyT2 immunolabeling was used to identify inhibitory glycinergic terminals of Golgi cells [30]. Double immunolabeling experiments revealed that α-synuclein is exclusively associated with VGluT1-positive ($VGluT1^+$) excitatory terminals (Fig. 3).

α-Synuclein in Granule Cell Synaptic Terminals of the Molecular Layer

At higher magnification, immunostaining with α-synuclein antibody revealed a homogenous punctate-like labeling of synaptic terminals (Fig. 3a–d). When sections were colabeled with antibodies recognizing VGluTs, we observed extensive colocalization of α-synuclein with VGluT1 in the granule cell

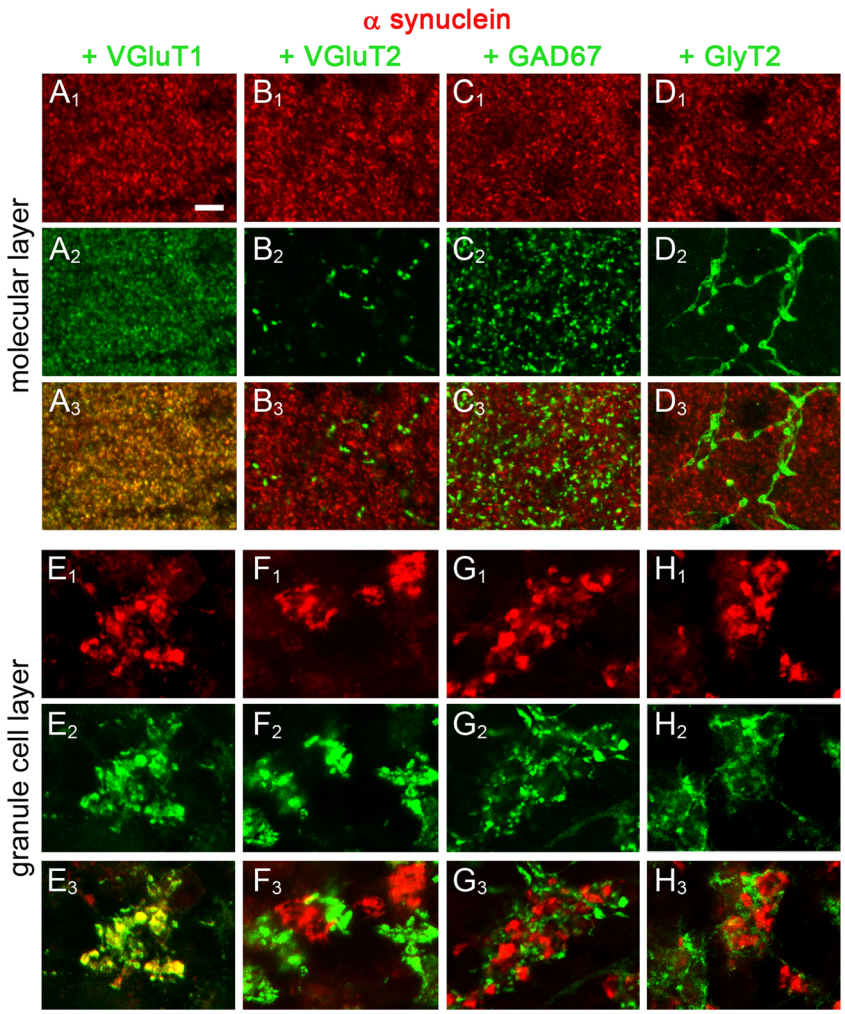

Fig. 3 α-Synuclein colocalizes with VGluT1 in cerebellar synaptic terminals. Double immunolabeling with α-synuclein (EnCor Biotechnology) and cell-type-specific marker antibodies. Images illustrate the immunostaining pattern in the molecular (**a**–**d**) and granule cell layer (**e**–**h**) of the nodulus. **a**–**d** In the molecular layer, the α-synuclein immunolabeling shows a distinct punctate immunolabeling of synaptic terminals ($\mathbf{a}_1$, $\mathbf{b}_1$, $\mathbf{c}_1$, $\mathbf{d}_1$). VGluT1 ($\mathbf{a}_2$) and VGluT2 ($\mathbf{b}_2$) immunostaining were used to visualize the excitatory synaptic terminals of granule cells and climbing fibers, respectively. GAD67 ($\mathbf{c}_2$) and GlyT2 ($\mathbf{d}_2$) label the inhibitory GABAergic and glycinergic terminals. Merged images in panels $\mathbf{a}_3$, $\mathbf{b}_3$, $\mathbf{c}_3$, and $\mathbf{d}_3$ show that only the $VGluT1^+$ granule cell terminals contain α-synuclein. **e**–**h** In the granule cell layer, the α-synuclein immunolabeling is exclusively localized to MFTs ($\mathbf{e}_1$, $\mathbf{f}_1$, $\mathbf{g}_1$, $\mathbf{h}_1$). VGluT1 ($\mathbf{e}_2$) and VGluT2 ($\mathbf{f}_2$) antibodies also label MFTs, while GAD67 ($\mathbf{g}_2$) and GlyT2 ($\mathbf{h}_2$) antibodies label the GABAergic and glycinergic terminals. Merged images in panels $\mathbf{e}_3$, $\mathbf{f}_3$, $\mathbf{g}_3$, and $\mathbf{h}_3$ show that only the $VGluT1^+$ MFTs contain α-synuclein. *Scale bars:* **a**–**h** 5 μm

terminals (Fig. 3a) but not with VGluT2, which labeled the synaptic terminals of climbing fibers (Fig. 3b). GAD67 antibody labeled the terminals of inhibitory neurons, but none of these terminals contained α-synuclein (Fig. 3c). Similarly, GlyT2$^+$ terminals were free of α-synuclein labeling (Fig. 3d). Based on these results, we conclude that α-synuclein is expressed by granule cells and that the protein is preferentially accumulated in the synaptic terminals.

α-Synuclein in MFTs of the Granule Cell Layer

In the granule cell layer, α-synuclein was distinctly associated with the MFTs (Figs. 2c–e and 3e–h). All α-synuclein-positive MFTs contained VGluT1, but not all VGluT1$^+$ MFTs contained α-synuclein. Figure 4 illustrates the differential distribution of the α-synuclein-positive and VGluT1$^+$ MFTs. In the nodulus and ventral uvula (folium IXc), most of the MFTs displayed both proteins (Fig. 4a), while in other lobules, the frequency of double labeling varied greatly (Fig. 4b–d). High densities of VGluT1$^+$/α-synuclein$^+$ MFTs were observed in lobules I (Fig. 4d), II, VIb, and VII, while in other lobules, only about one fourth of VGluT1$^+$ MFTs displayed α-synuclein (Fig. 4b). We have previously described a narrow area between folium IXa and IXb, which is defined by the absence of UBCs and their terminals [18]. This "no UBC zone" was also easily recognized in α-synuclein-immunolabeled sections by the obvious lack of immunolabeling (Figs. 2a, b and 4b).

Distribution of VGluT1 and VGluT2 is complementary in most brain structures with the exception of a few brain areas in which neurons coexpressing both proteins were reported [31–34]. Among the neuronal structures in which these two transporters colocalize are the MFTs in the cerebellum [27, 28, 32]. Notably, only a subset of MFTs contains both VGluT1 and VGluT2 and the frequency of these double-labeled MFTs varies in different cerebellar lobules [28]. In line with these observations, we found that most MFTs displayed either α-synuclein or VGluT2 staining (Figs. 3f and 5). Only a small subset of α-synuclein$^+$ MFTs displayed a faint VGluT2 immunostaining (Fig. 5). In lobule X, we observed very few double immunostained α-synuclein$^+$/VGluT2$^+$ MFTs (Fig. 5a), while the double-labeled terminals were more frequent in lobules I, VIb, and VIII (Fig. 5b, c). Because all α-synuclein-positive MFTs contained VGluT1, it can be inferred that the observed α-synuclein$^+$/VGluT2$^+$ MFTs probably also contain VGluT1. GABAergic and glycinergic terminals in the granule cell layer did not contain α-synuclein (Fig. 3g, h).

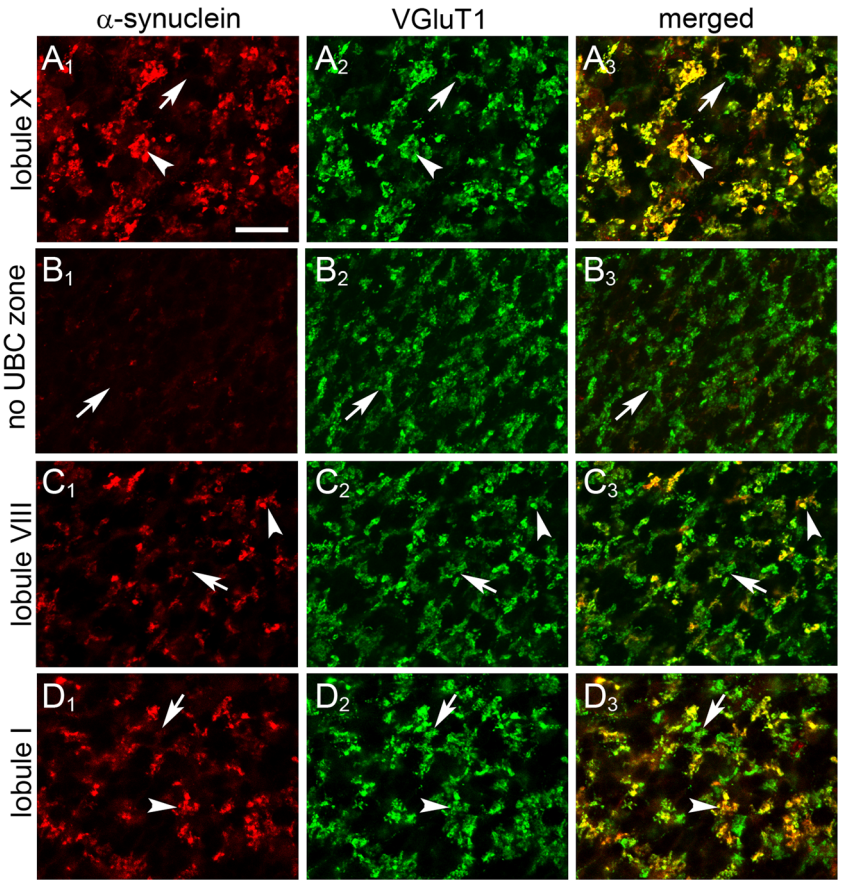

Fig. 4 Distribution of α-synuclein$^+$ and VGluT1$^+$ MFTs in different cerebellar regions. **a–d** Single color images illustrate the distribution of the α-synuclein$^+$ (**a**$_1$–**d**$_1$) and VGluT1$^+$ (**a**$_2$–**d**$_2$) MFTs. Merged images (**a**$_3$–**d**$_3$) show that all α-synuclein-labeled MFTs contain VGluT1 (*arrowheads*) but not all VGluT1$^+$ MFTs contain α-synuclein (*arrows*). In the nodulus (*lobule X*), almost all MFTs display both proteins (**a**). In contrast, the transition area between folium IXa and IXb (*no UBC zone*) lacks α-synuclein labeling (**b**). *Scale bars:* **a–d** 20 μm

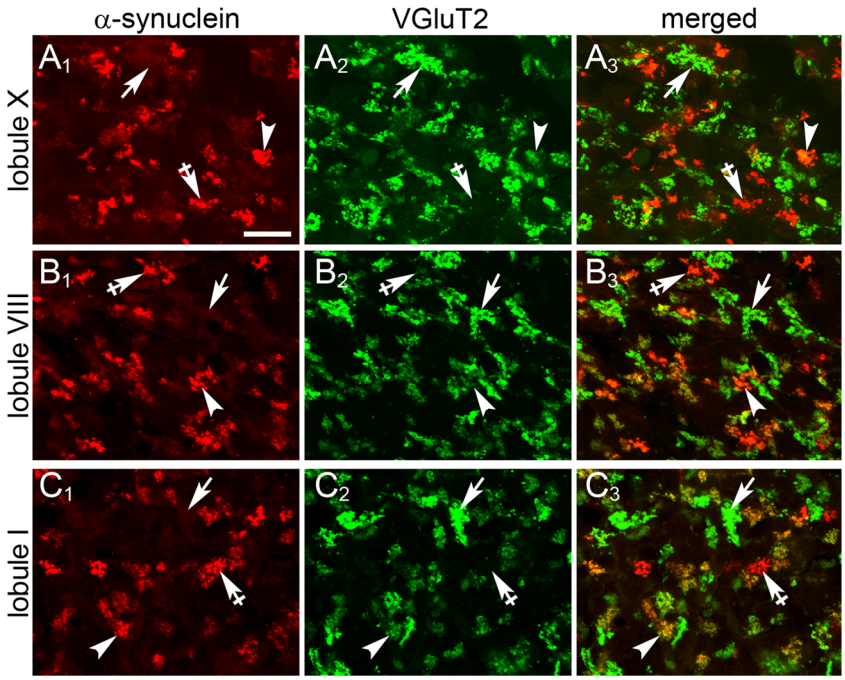

Fig. 5 Distribution of α-synuclein$^+$ and VGluT2$^+$ MFTs in different cerebellar regions. **a**–**c** Single color images illustrate the distribution of the α-synuclein$^+$ (**a**$_1$–**c**$_1$) and VGluT2$^+$ (**a**$_2$–**c**$_2$) MFTs. Merged images (**a**$_3$–**c**$_3$) show that most MFTs display either α-synuclein (*crossed arrow*) or VGluT2 (*arrows*). Lobule X (**a**$_3$) contains only a few α-synuclein$^+$ and VGluT2$^+$ double-labeled MFTs (*arrowhead*). About half of the α-synuclein$^+$ MFTs are VGluT2$^+$ in lobule VIII (**b**$_3$), while in lobule I (**c**$_3$), most α-synuclein$^+$ MFTs contain VGluT2. *Scale bars:* **a**–**c** 20 μm

α-Synuclein in Cerebellar UBCs

Our data show that α-synuclein is associated with excitatory terminals including a subset of MFTs in the granule cell layer. The cerebellar granule cell layer contains two distinct mossy fiber systems: the canonical mossy fiber system of afferent fibers originating from the precerebellar nuclei and the intrinsic mossy fiber system formed by the axons of UBCs [17]. UBC axons often terminate in the same lobule where their parent soma are located [17, 35], and therefore, the vestibulocerebellum contains the highest concentration of intrinsic MFTs. Nunzi and Mugnaini [21] estimated that about 50 % of MFTs in the vestibulocerebellum are provided by UBCs.

The distribution of α-synuclein labeling in the granule cell layer of the vestibulocerebellum was reminiscent of the typical UBC distribution pattern (compare Figs. 2a, b and 6a; see also [18]), e.g., intense immunolabeling in nodulus and folium IXc, moderate labeling in folium IXb, and faint to moderate immunolabeling in the rest of the cerebellum with the exception of the transition zone between IXa and IXb, where the immunolabeling was absent (Figs. 2a, b and 6c, d). MFTs of both UBC types contain VGluT1 [29]. In the nodulus, α-synuclein and VGluT1 colocalized in MFTs (Fig. 4a) indicating the presence of α-synuclein in UBC terminals. UBCs are classified in two subclasses on the basis of size, distribution, electrophysiological properties, and expression of selective markers [18, 36, 37]. To identify the UBC population expressing α-synuclein, we employed double immunostaining with UBC-type-specific markers. Type I UBCs were visualized by calretinin antibody (Figs. 6c and 7a, b). This immunostaining

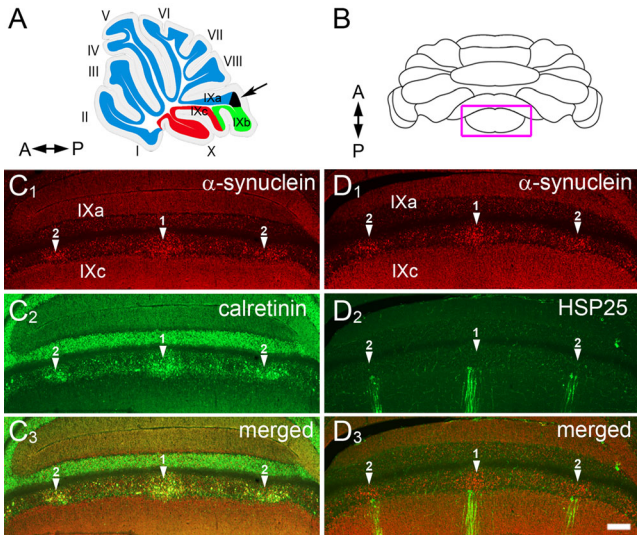

Fig. 6 α-Synuclein is expressed in zonal compartments in the adult mouse cerebellum. **a** A distribution map of UBC in mouse cerebellum. The highest densities of both UBC types are found in lobule X and folium IXc (*red area*). Folium IXb contains mostly type II UBCs (*green area*). Few UBCs are found in the rest of the cerebellar lobules (*blue colored areas*) with the exception of the transition zone between folium IXa and IXb where no UBCs are found (*black area*; *arrow*). Anterior (*A*) and posterior (*P*) directions are indicated by a *double-headed arrow*. **b** Schematic diagram of the cerebellum shown in whole mount. The *red box* denotes the region shown in panels **c** and **d**. **c**, **d** α-Synuclein-labeled zonal "clusters" in the granular layer of lobule IX (**c**$_1$, **d**$_1$) align with either calretinin immunoreactive UBC clusters (**c**$_2$, **c**$_3$) or Hsp25$^+$ Purkinje cell zones (**d**$_2$, **d**$_3$). Notably, the boundaries of the α-synuclein$^+$ clusters are not as sharply defined as the Purkinje cell zones (**d**$_3$). The midline and lateral zones are labeled as 1 and 2, respectively (*arrowheads*). *Scale bar*, 125 μm

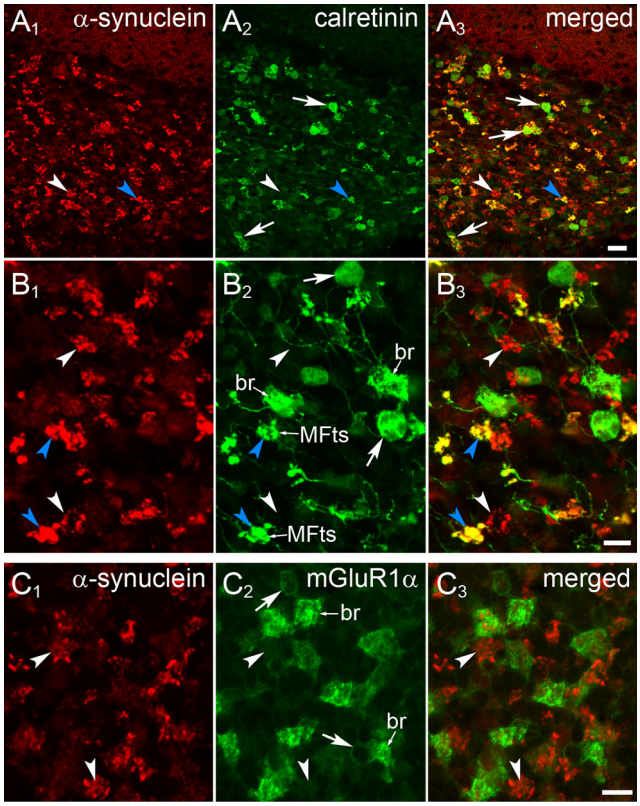

Fig. 7 α-Synuclein in the axonal terminals of UBCs. **a**, **b** Type I UBCs (*arrows*) are visualized with calretinin immunolabeling. This staining afforded labeling of all UBC compartments (**b**$_2$); soma (*arrows*), dendritic brush (*br*), and axon including the synaptic terminals (MFTs; *blue arrowheads*). All calretinin$^+$ MFTs contain α-synuclein (*blue arrowheads*); however, many α-synuclein$^+$ MFTs (*white arrowheads*) do not express calretinin. **c** Type II UBCs are visualized by mGluR1α immunolabeling. This staining labels only the soma (*arrows*) and the dendritic brush (*br*). Double immunolabeling with α-synuclein shows the presence of α-synuclein$^+$ MFTs (*arrowheads*) in areas that are rich with type II UBCs. *Scale bar*, **a**$_{1–3}$ 20 μm; **b**$_{1–3}$ 10 μm; **c**$_{1–3}$ 10 μm

resulted in labeling of all cytoplasmic compartments including the soma, dendritic brush, axon, and MFTs (Fig. 7b$_2$). Notably, α-synuclein showed a striped pattern in folium IXc that was in register with UBC-rich stripes visualized by calretinin immunolabeling (Fig. 6b, c; [18, 38]) as well as with Hsp25$^+$ Purkinje cell bands (Fig. 6d; [39, 40]). Double labeling experiments revealed that all calretinin$^+$ MFTs contained α-synuclein. These double-labeled MFTs represented only about one third of all α-synuclein$^+$ MFTs. Type II UBCs were labeled with mGluR1α antibody (Fig. 7c), and although this antibody is a reliable marker for type II UBCs, it only labeled their dendritic brushes and somata (Fig. 7c$_2$); thus, in double immunostaining experiments, α-synuclein-labeled terminals could not be unequivocally assigned to type II UBCs (Fig. 7c). However, the presence of numerous α-synuclein$^+$/calretinin$^-$/VGluT1$^+$ MFTs indicates that not only type I but also type II UBCs contain α-synuclein.

α-Synuclein in MFTs of Type I and Type II UBCs In Vitro

Our data suggest that both UBC types express α-synuclein. Yet, we cannot exclude that the α-synuclein$^+$/calretinin$^-$ (also VGluT1$^+$) MFTs represent extrinsic mossy fibers and, thus, do not belong to type II UBCS.

To address this problem, we utilized organotypic slice cultures prepared from the P8-P10 cerebellar nodulus. In these cultures, the extrinsic mossy fibers degenerate, while both types of UBCs survive long term—up to 30 DIV—and form an intricate mossy fiber network [21, 29]. In the current study, nodular slices were cultured for 22–24 DIV. Immunohistochemical analysis confirmed that both UBC subtypes were present in these cultures. Type I and type II UBCs were visualized by calretinin (Fig. 8a) and mGluR1α (Fig. 8b) immunostaining, respectively. Consistent with our tissue staining experiments, we found that calretinin labeled the MFTs of type I UBCs. These terminals also contained α-synuclein (Fig. 8a). However, the majority of α-synuclein$^+$ MFTs lacked calretinin immunolabeling. Because in these cultures the only source of MFTs are the UBCs, we can conclude that both UBC types contain α-synuclein.

α-Synuclein in UBC-Deficient Moonwalker Mouse

Our experiments show expression of α-synuclein in type II UBCs in vitro; however, neurons under artificial conditions may express proteins that they do not produce in vivo. For example, type I UBCs were shown to contain VGluT2 in organotypic cultures [29], yet we were unable to confirm this finding in cerebellar cryosections. In lobule X, only a few calretinin$^+$ MFTs contained faint VGluT2 immunolabeling (not shown). This result is consistent with the ISH data published on the Allen brain atlas [15] showing no VGluT2 ISH signal in the cerebellum. This observation prompted us to further investigate the presence of α-synuclein in type II UBCs in vivo.

To this end, we took advantage of *Mwk* mutant mice, in which type II UBCs are completely ablated by 1 month of age (in Fig. 9 compare panel a with panel b; [20]). Type I UBCs are still found in these mice, but their number is reduced dramatically (in Fig. 9 compare panel c with panel d; [20]). When cerebellar sections from *Mwk* mice were labeled with α-synuclein, we found a dramatic decrease in α-synuclein$^+$ MFTs (Fig. 9e–h) in lobule X and ventral IX. The distribution of the α-synuclein MFTs in these lobules was in register with the distribution of calretinin$^+$ UBCs and their terminals (compare panels f and d in Fig. 9). Double immunostaining with calretinin and α-synuclein revealed an almost complete colocalization of these two proteins in the remaining MFTs (Fig. 10). These results further support the conclusion that both cell types—type I and type II UBCs—express α-synuclein.

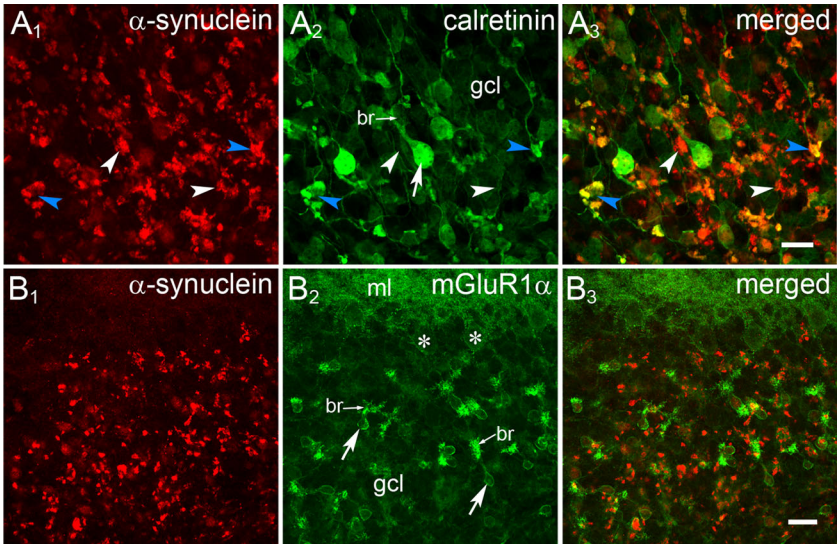

Fig. 8 α-Synuclein is expressed in intrinsic MFTs in vitro. Organotypic slice cultures of the mouse nodulus grown for 24 DIV and double immunolabeled with α-synuclein (EnCor Biotechnology) and UBC type specific markers. **a**, **b** Type I UBCs (*arrows*) are visualized with calretinin immunolabeling. This staining visualizes all UBC compartments (**b**$_2$); soma (*arrows*), dendritic brush (*br*), and axon including the synaptic terminals (MFTs; *blue arrowheads*). All calretinin$^+$ MFTs contain α-synuclein (*blue arrowheads*); however, many α-synuclein$^+$ MFTs (*white arrowheads*) do not express calretinin. **c** Type II UBC are visualized by mGluR1α immunolabeling. This staining labels only the soma (*arrows*) and dendritic brush (*br*) of UBCs. Double immunolabeling with α-synuclein shows MFTs (*arrowheads*) in areas that are rich with type II UBCs. *Scale bar*, **a**$_{1–3}$ 20 μm; **b**$_{1–3}$ 10 μm; **c**$_{1–3}$ 10 μm

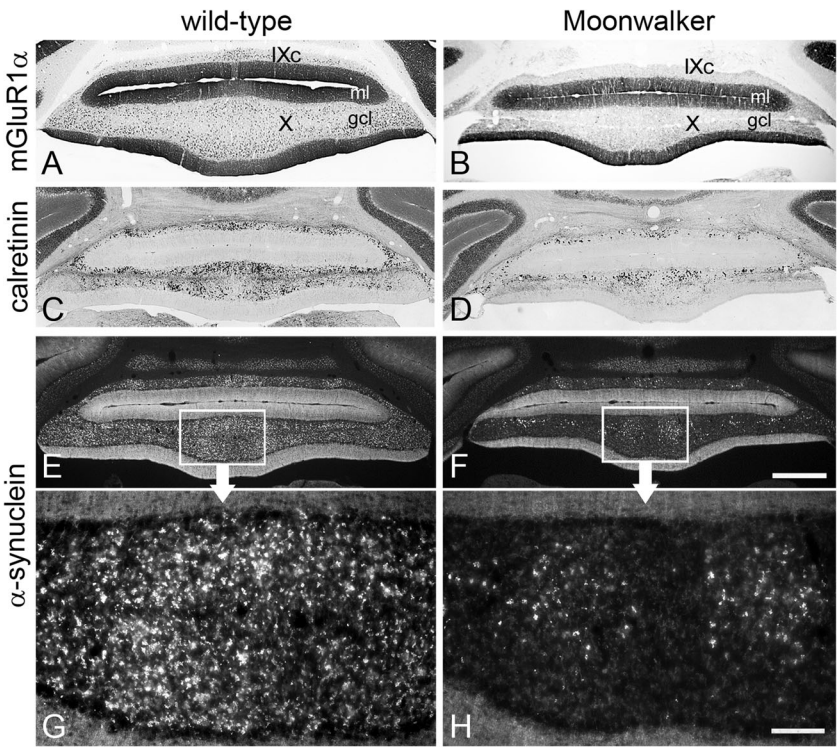

Fig. 9 Reduced α-synuclein immunolabeling in 1-month-old *Mwk* mutant mouse correlates with the loss of UBCs. **a**–**d** mGluR1α (**a**, **b**) and CR (**c**, **d**) immunoperoxidase labeling of type II UBCs and type I UBCs, respectively. Comparison of wild-type (**a**, **c**) and *Mwk* (**b**, **d**) mice coronal sections taken from the same brain areas reveals the absence of GluR1α$^+$ type II UBCs (**b**) and severe depletion of calretinin$^+$ type I UBCs (**d**) from the granule cell layer (*gcl*) of the nodulus (*lobule X*) and folium IXc. The Purkinje cell arbors in the molecular layer (*ml*) show distinct mGluR1α labeling (**a**, **b**). **e**–**h** α-Synuclein immunofluorescence labeling of wild-type (**e**, **g**) and *Mwk* (**f**, **h**) mice. The *Mwk* nodulus (**f**, **h**) contains significantly less α-synuclein$^+$ MFTs than the wild-type nodulus (**e**, **g**). **g**, **h** Enlarged magnifications of the *boxed images* in **e** and **f**, respectively. *Scale bar*, **a**–**f** 500 μm; **g**, **h** 100 μm

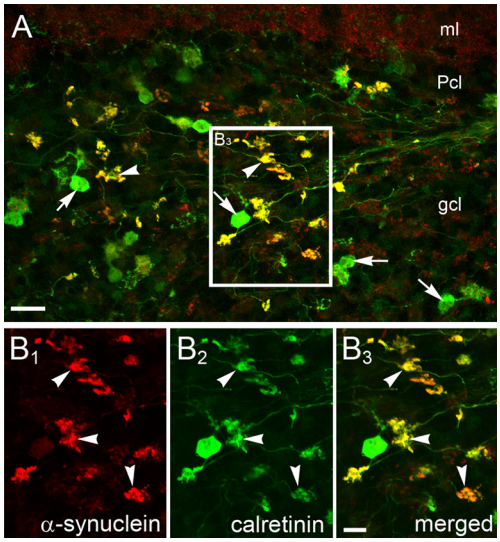

Fig. 10 α-Synuclein and calretinin are colocalized in MFTs in the nodulus of 1-month-old *Mwk* mutant mouse. At this age, only a few calretinin$^+$ UBCs (*arrows*) are present. *Arrowheads* point to α-synuclein$^+$/calretinin$^+$ profiles in MFTs. Panel $\mathbf{b}_3$ is an enlarged image of the *boxed area* in panel **a**. *Scale bar*, **a** 20 μm; $\mathbf{b}_{1-3}$ 10 μm

Discussion

This study shows that α-synuclein is present in cerebellar glutamatergic terminals. In the molecular layer, α-synuclein is present in the granule cell terminals, while in the granule cell layer, α-synuclein is associated with MFTs. Moreover, we show that α-synuclein is especially enriched in the intrinsic MFTs (the terminals of UBC axons). Consistent with this observation, α-synuclein is dramatically decreased in the vestibulocerebellum of the *Mwk* mouse, a model of cerebellar ataxia in which UBCs are almost completely ablated.

Previously, it has been shown that α-synuclein-containing terminals are localized in both the molecular and the granule cell layers [27, 28, 34], yet the origin of these terminals had not been determined. Here we took advantage of cell-type-specific markers recognizing glutamatergic (VGluT1 and VGluT2; VGluT3 is not present in the cerebellum [41]), GABAergic, and glycinergic terminals to identify the nature of the synuclein-positive terminals in the cerebellum. We found that only the glutamatergic terminals contain α-synuclein. Similar findings were reported in the hippocampus where the excitatory, but not the inhibitory, neurons were found to express α-synuclein [16]. Our data showing that synuclein is selectively present in glutamatergic terminals supports previous findings showing that α-synuclein promotes SNARE complex formation at the presynaptic membranes [10, 12]. Importantly, the SNARE proteins are not expressed in GABAergic terminals (with the exception of the terminals of basket cells [42]), and the soluble NSF attachment protein-25 (SNAP-25, a component of the SNARE complex) has been also associated with glutamatergic but not GABAergic synapses [43, 44].

Intriguingly, we found that VGluT1 is coexpressed with α-synuclein in cerebellar synaptic terminals. On the other hand, VGluT2 expressing climbing fibers and a majority of MFTs do not contain α-synuclein. Our data indicate that the α-synuclein$^+$/VGluT2$^+$ MFTs represent a subset of the VGluT1$^+$ MFTs based on pieces of evidence: (1) all α-synuclein$^+$ MFTs express VGluT1 and (2) VGluT1 and VGulT2 are coexpressed in a small subset of MFTs [27, 28, 32]. VGluT1 and VGluT2 exhibit a complementary expression pattern in the CNS with few exceptions [27, 34]. However, the physiological significance of the differential expression of these transporters is still unknown. Fremeau and colleagues [31] suggested that the glutamate transporters differentially affect glutamate packaging and release. They proposed that VGluT1 expression is dominant in synapses with low probability release, like in the parallel fibers, while VGluT2 expression may correlate with high probability release, for example in climbing fibers [45]. Our data however show that MFTs are heterogeneous with regard to VGluT expression, as they can express VGluT1, VGluT2 or, in a small subset, both these transporters. Thus, it may be suggested that release probability varies between different MFTs; this latter hypothesis is in line with the observation of large fiber-to-fiber variation in MF synaptic strength [46]. Interestingly, in the vestibulocerebellum of *Mwk* mice, in which UBCs are absent, VGLUT1 expression is decreased, thus suggesting that intrinsic MFTs preferentially express this transporter, which may suggest that intrinsic MFs form synapses with lower release probability than extrinsic MFTs. α-Synuclein, however, is also enriched in UBC axons. It was suggested that loss of α-synuclein reduces synaptic efficacy at the Schaeffer collateral-CA1 synapse [47], implying that its presence in presynaptic sites correlates with high release probability. However, further targeted electrophysiological recordings will be required to ascertain whether intrinsic UBC MFs are high or low probability synapses.

Our data, on the other hand, may indirectly provide some hints as to the functional roles of UBCs. MSA-C is characterized by synuclein inclusions in glia as well as by neuronal cell death and ubiquitin-positive neuritic degeneration, which is particularly pronounced in the vermis [48], a UBC-rich area [18]. Because UBC terminals are enriched in α-synuclein, it may be suggested that, similar to the moonwalker ataxia [20], MSA-C may also be characterized by severe UBC loss. It would be interesting to test this hypothesis on human samples. A positive finding may further support the idea that UBC loss is important for the development of ataxia.

Acknowledgments This study was funded by NIH grant NS09904 (MM), U54HD083092 (RVS), and NS089664 (RVS). The BCM IDDRC Neuropathology Core performed a portion of the staining experiments.

The content is solely the responsibility of the authors and does not necessarily represent the official views of the NIH.

Conflict of Interest The authors declare that they have no conflict of interest.

References

1. Bendor JT, Logan TP, Edwards RH. The function of alpha-synuclein. Neuron. 2013;79:1044–66.
2. Clayton DF, George JM. Synucleins in synaptic plasticity and neurodegenerative disorders. J Neurosci Res. 1999;58:120–9.
3. Lin DJ, Hermann KL, Schmahmann JD. Multiple system atrophy of the cerebellar type: clinical state of the art. Mov Disord. 2014;29:294–304.
4. Marques O, Outeiro TF. Alpha-synuclein: from secretion to dysfunction and death. Cell Death Dis. 2012;3, e350.
5. Sebeo J, Hof PR, Perl DP. Occurrence of alpha-synuclein pathology in the cerebellum of Guamanian patients with parkinsonism-dementia complex. Acta Neuropathol. 2004;107:497–503.
6. Surguchov A. Synucleins: are they two-edged swords? J Neurosci Res. 2013;91:161–6.
7. Cheng F, Vivacqua G, Yu S. The role of alpha-synuclein in neurotransmission and synaptic plasticity. J Chem Neuroanat. 2011;42:242–8.
8. Diao J, Burré J, Vivona S, Cipriano DJ, Sharma M, Kyoung M, et al. Native alpha-synuclein induces clustering of synaptic-vesicle mimics via binding to phospholipids and synaptobrevin-2/VAMP2. Elife. 2013;2, e00592.
9. Scott D, Roy S. Alpha-synuclein inhibits intersynaptic vesicle mobility and maintains recycling-pool homeostasis. J Neurosci. 2012;32:10129–35.
10. Südhof TC, Rizo J. Synaptic vesicle exocytosis. Cold Spring Harb Perspect Biol. 2011;3.
11. Vargas KJ, Makani S, Davis T, Westphal CH, Castillo PE, Chandra SS. Synucleins regulate the kinetics of synaptic vesicle endocytosis. J Neurosci. 2014;34:9364–76.
12. Burré J, Sharma M, Südhof TC. Alpha-synuclein assembles into higher-order multimers upon membrane binding to promote SNARE complex formation. Proc Natl Acad Sci U S A. 2014;111:E4274–83.
13. Wang L, Das U, Scott DA, Tang Y, McLean PJ, Roy S. Alpha-synuclein multimers cluster synaptic vesicles and attenuate recycling. Curr Biol. 2014;24:2319–26.
14. Li J, Henning Jensen P, Dahlström A. Differential localization of alpha-, beta- and gamma-synucleins in the rat CNS. Neuroscience. 2002;113:463–78.
15. Lein ES, Hawrylycz MJ, Ao N, Ayres M, Bensinger A, Bernard A, et al. Genome-wide atlas of gene expression in the adult mouse brain. Nature. 2007;445:168–76.
16. Taguchi K, Watanabe Y, Tsujimura A, Tatebe H, Miyata S, Tokuda T, et al. Differential expression of alpha-synuclein in hippocampal neurons. PLoS ONE. 2014;9, e89327.
17. Mugnaini E, Sekerková G, Martina M. The unipolar brush cell: a remarkable neuron finally receiving deserved attention. Brain Res Rev. 2011;66:220–45.
18. Sekerková G, Watanabe M, Martina M, Mugnaini E. Differential distribution of phospholipase C beta isoforms and diaglycerol kinase-beta in rodents cerebella corroborates the division of unipolar brush cells into two major subtypes. Brain Struct Funct. 2014;219:719–49.
19. Becker EB, Oliver PL, Glitsch MD, Banks GT, Achilli F, Hardy A, et al. A point mutation in TRPC3 causes abnormal Purkinje cell development and cerebellar ataxia in moonwalker mice. Proc Natl Acad Sci U S A. 2009;106:6706–11.
20. Sekerková G, Kim JA, Nigro MJ, Becker EB, Hartmann J, Birnbaumer L, et al. Early onset of ataxia in moonwalker mice is accompanied by complete ablation of type II unipolar brush cells and Purkinje cell dysfunction. J Neurosci. 2013;33:19689–94.
21. Nunzi MG, Mugnaini E. Unipolar brush cell axons form a large system of intrinsic mossy fibers in the postnatal vestibulocerebellum. J Comp Neurol. 2000;422:55–65.
22. Fong AY, Stornetta RL, Foley CM, Potts JT. Immunohistochemical localization of GAD67-expressing neurons and processes in the rat brainstem: subregional distribution in the nucleus tractus solitarius. J Comp Neurol. 2005;493:274-90.
23. Milanese M, Romei C, Usai C, Oliveri M, Raiteri L. A new function for glycine GlyT2 transporters: Stimulation of γ-aminobutyric acid release from cerebellar nerve terminals through GAT1 transporter reversal and Ca(2+)-dependent anion channels. J Neurosci Res. 2014;92:398-408.
24. Nunzi MG, Mugnaini E. Aspects of the neuroendocrine cerebellum: expression of secretogranin II, chromogranin A and chromogranin B in mouse cerebellar unipolar brush cells. Neuroscience. 2009;162:673–87
25. Ramirez EP, Vonsattel JP. Neuropathologic changes of multiple system atrophy and diffuse Lewy body disease. Semin Neurol. 2014;34:210–6.
26. Hirohata M, Ono K, Morinaga A, Ikeda T, Yamada M. Cerebrospinal fluid from patients with multiple system atrophy promotes in vitro alpha-synuclein fibril formation. Neurosci Lett. 2011;491:48–52.
27. Hioki H, Fujiyama F, Taki K, Tomioka R, Furuta T, Tamamaki N, et al. Differential distribution of vesicular glutamate transporters in the rat cerebellar cortex. Neuroscience. 2003;117:1–6.
28. Hisano S, Sawada K, Kawano M, Kanemoto M, Xiong G, Mogi K, et al. Expression of inorganic phosphate/vesicular glutamate transporters (BNPI/VGLUT1 and DNPI/VGLUT2) in the cerebellum and precerebellar nuclei of the rat. Brain Res Mol Brain Res. 2002;107:23–31.
29. Nunzi MG, Russo M, Mugnaini E. Vesicular glutamate transporters VGLUT1 and VGLUT2 define two subsets of unipolar brush cells in organotypic cultures of mouse vestibulo cerebellum. Neuroscience. 2003;122:359–71.
30. Simat M, Parpan F, Fritschy JM. Heterogeneity of glycinergic and gabaergic interneurons in the granule cell layer of mouse cerebellum. J Comp Neurol. 2007;500:71–83.
31. Fremeau Jr RT, Voglmaier S, Seal RP, Edwards RH. VGLUTs define subsets of excitatory neurons and suggest novel roles for glutamate. Trends Neurosci. 2004;27:98–103.
32. Ge SN, Li ZH, Tang J, Ma Y, Hioki H, Zhang T, et al. Differential expression of VGLUT1 or VGLUT2 in the trigeminothalamic or trigeminocerebellar projection neurons in the rat. Brain Struct Funct. 2014;219:211–29.
33. Kaneko T, Fujiyama F. Complementary distribution of vesicular glutamate transporters in the central nervous system. Neurosci Res. 2002;42:243–50.
34. Kaneko T, Fujiyama F, Hioki H. Immunohistochemical localization of candidates for vesicular glutamate transporters in the rat brain. J Comp Neurol. 2002;444:39–62.
35. Berthié B, Axelrad H. Granular layer collaterals of the unipolar brush cell axon display rosette-like excrescences. A Golgi study in the rat cerebellar cortex. Neurosci Lett. 1994;167:161–5.
36. Kim JA, Sekerková G, Mugnaini E, Martina M. Electrophysiological, morphological, and topological properties of two histochemically distinct subpopulations of cerebellar unipolar brush cells. Cerebellum. 2012;1012–25.
37. Nunzi MG, Shigemoto R, Mugnaini E. Differential expression of calretinin and metabotropic glutamate receptor mGluR1alpha

defines subsets of unipolar brush cells in mouse cerebellum. J Comp Neurol. 2002;451:189–99.
38. Chung SH, Sillitoe RV, Croci L, Badaloni A, Consalez G, Hawkes R. Purkinje cell phenotype restricts the distribution of unipolar brush cells. Neuroscience. 2009;164:1496–508.
39. Armstrong CL, Krueger-Naug AM, Currie RW, Hawkes R. Constitutive expression of the 25-kDa heat shock protein Hsp25 reveals novel parasagittal bands of Purkinje cells in the adult mouse cerebellar cortex. J Comp Neurol. 2000;416:383–97.
40. Armstrong CL, Krueger-Naug AM, Currie RW, Hawkes R. Expression of heat-shock protein Hsp25 in mouse Purkinje cells during development reveals novel features of cerebellar compartmentation. J Comp Neurol. 2001;429:7–21.
41. Gras C, Herzog E, Bellenchi GC, Bernard V, Ravassard P, Pohl M, et al. A third vesicular glutamate transporter expressed by cholinergic and serotoninergic neurons. J Neurosci. 2002;22:5442–51.
42. Benagiano V, Lorusso L, Flace P, Girolamo F, Rizzi A, Bosco L, et al. VAMP-2, SNAP-25A/B and syntaxin-1 in glutamatergic and GABAergic synapses of the rat cerebellar cortex. BMC Neurosci. 2011;12:118.
43. Garbelli R, Inverardi F, Medici V, Amadeo A, Verderio C, Matteoli M, et al. Heterogeneous expression of SNAP-25 in rat and human brain. J Comp Neurol. 2008;506:373–86.
44. Verderio C, Pozzi D, Pravettoni E, Inverardi F, Schenk U, Coco S, et al. SNAP-25 modulation of calcium dynamics underlies differences in GABAergic and glutamatergic responsiveness to depolarization. Neuron. 2004;41:599–610.
45. Dittman JS, Regehr WG. Calcium dependence and recovery kinetics of presynaptic depression at the climbing fiber to Purkinje cell synapse. J Neurosci. 1998;18:6147–62.
46. Sargent PB, Saviane C, Nielsen TA, DiGregorio DA, Silver RA. Rapid vesicular release, quantal variability, and spillover contribute to the precision and reliability of transmission at a glomerular synapse. J Neurosci. 2005;25:8173–87.
47. Martín ED, González-García C, Milán M, Fariñas I, Ceña V. Stressor-related impairment of synaptic transmission in hippocampal slices from alpha-synuclein knockout mice. Eur J Neurosci. 2004;20:3085–91.
48. Lantos PL. The definition of multiple system atrophy: a review of recent developments. J Neuropathol Exp Neurol. 1998;57:1099–111.